

The mRNA-binding protein Serbp1 as an auxiliary protein associated with mammalian cytoplasmic ribosomes

Akiko Muto, Yoshihiko Sugihara, Minami Shibakawa, Kenzi Oshima, Tsukasa Matsuda, and Daita Nadano\*

*Department of Applied Molecular Biosciences, Graduate School of Bioagricultural Sciences, Nagoya University, Nagoya 464-8601, Japan*

Short title: Serbp1 in mammalian cytoplasmic ribosomes

---

\* Correspondence to:

Daita Nadano, Ph. D.

Associate Professor

Department of Applied Molecular Biosciences

Graduate School of Bioagricultural Sciences

Nagoya University

Furo-cho, Chikusa, Nagoya 464-8601, Japan

Phone: +81-52-789-4130; Fax: +81-52-789-4128

E-mail: nadano@agr.nagoya-u.ac.jp

## Abstract

While transcription plays an obviously important role in gene expression, translation has recently been emerged as a key step that defines the composition and quality of the proteome in the cell of higher eukaryotes including mammals. Selective translation is supposed to be regulated by the structural heterogeneity of cytoplasmic ribosomes including differences in protein composition and chemical modifications. However the current knowledge on the heterogeneity of mammalian ribosomes is limited. Here we report mammalian Serbp1 as a ribosome-associated protein. The translated products of Serbp1 gene, including the longest isoform, were found to be localized in the nucleolus as well as in the cytoplasm. Subcellular fractionation indicated that most of cytoplasmic Serbp1 molecules were precipitated by ultracentrifugation. Proteomic analysis identified Serbp1 in the cytoplasmic ribosomes of the rodent testis. Polysome profiling suggested that Serbp1, as a component of the small 40S subunit, was included in translating ribosomes (polysomes). Co-sedimentation of Serbp1 with the 40S subunit was observed after dissociation of the ribosomal subunits. Serbp1 was also included in the ribosomes of human cancer cells, which may lead to a mechanistic understanding of an emerging link between Serbp1 and tumor progression.

Keywords: cytoplasmic ribosome, gene expression, isoform, malignant tumor, mammal, mRNA-binding protein, polysome, translational control

## 1 INTRODUCTION

Complete sequencing of mammalian genomes has identified the precise number of genes per genome. Human genome has been reported to include about 21,000 genes, which was surprisingly small since the total gene number had been believed to be around 100,000 for a long time [1]. The ‘missing’ complexity has been considered to be explained, in part, by alternative splicing, the process by which multiple different functional mRNAs can be synthesized from one gene [2].

Regulation of gene expression in eukaryotic cells is a multilayer process and classically divided into transcriptional and post-transcriptional steps. RNA-binding proteins have been recognized as crucial players in the post-transcriptional step. Human genome has been estimated to contain 1,542 RNA-binding proteins [3]. Nonetheless, the roles of these proteins in gene regulation are still far from complete understanding [4].

Serbp1 (also known as CGI-55 and PAI-RBP1) has first been identified by screening of proteins bound to plasminogen activator inhibitor type 1 (PAI-1) mRNA in rat hepatoma cells [5]. Serbp1 binds to the cyclic nucleotide-response sequence in the 3' -region of PAI-1 mRNA and regulates the stability of the transcript. It has been proposed that nuclear Serbp1 stabilizes PAI-1 mRNA and that cytoplasmic Serbp1 destabilizes it [6]. Subsequent to these studies, mammalian Serbp1 has been reported to be involved in DNA cleavage and recombination [7], chromatin remodeling [8], transcription [9], and cytoplasmic progesterone signaling via interaction with cell surface progesterin receptors [10]. Therefore, although there are more than a thousand RNA-binding proteins in mammals, Serbp1 has unique properties playing multiple roles inside and outside the nucleus of the cell. The nuclear-cytoplasmic distribution of Serbp1 has been proposed to be regulated by PRMT1-mediated arginine methylation [11].

As described above, one of the main functions of RNA-binding proteins is post-transcriptional gene regulation. In addition to the regulation of mRNA stability, previous studies have pointed out that other mechanisms are likely to be involved in post-transcriptional regulation by Serbp1. For example, Serbp1 promoted the inclusion of target mRNA in polysomes and its translation [12]. Serbp1-mediated translational control has also been suggested by another group [13]. The knowledge of Serbp1 in translation remains scarce. In the present report, we have analyzed the localization of Serbp1 in rodent and human cells and found the association of Serbp1 with cytoplasmic

ribosomes.

## 2. MATERIALS AND METHODS

### 2.1. Ethical statement

This study was approved by the Institutional Animal Care and Use Committee of Nagoya University and by the Institutional Safety Committee for Recombinant DNA Experiments of Nagoya University.

### 2.2 RNA preparation and reverse transcription (RT)-polymerase chain reaction (PCR)

Total RNA was prepared from the tissues of adult male BALB/c mice by using Trizol reagent (Invitrogen, Carlsbad, CA). Isolated RNA was treated with deoxyribonuclease and subjected to RT as described previously [14].

Partial cDNA (129 bp) of mouse Serbp1 (common to all four isoforms) was amplified by PCR from the total cDNAs of the mouse tissues. Amplification was carried as follows: denaturation at 94°C for 1 min and 25 cycles of denaturation at 94°C for 1 min, annealing at 60°C for 1 min, and extension at 72°C for 1 min. PCR primers were: 5'-CGATGGACAATGGAAAAAGG-3' (forward) and 5'-GCGGCCTAAGTCTCCAAAAT-3' (reverse). Partial cDNA of mouse glyceraldehyde-3-phosphate dehydrogenase (GAPDH) was amplified by the same cycle conditions as describe above, except for altering the cycle number from 25 to 20. Primers for GAPDH are described in our previous report [15]. Amplified DNAs were subjected to agarose gel electrophoresis followed by ethidium bromide staining.

### 2.3 Expression plasmids

The cDNA encoding the full-length mouse Serbp1 was amplified by PCR from mouse testis cDNA and cloned in-frame into the pEGFP-C1 and pEGFP-N3 plasmids (Clontech, Mountain View, CA) to express the protein bearing N-terminally and C-terminally fused green fluorescent proteins (GFP) in mammalian cells, respectively. The forward and reverse primers for cloning into pEGFP-C1 were 5'-TTTCTCGAGGGGATGCCTGGGCACCTACAGG-3' (XhoI site underlined) and 5'-TTTGAATCTTAGGCCAGAGCTGGGAAG-3' (EcoRI site underlined),

respectively. The forward and reverse primers for cloning into pEGFP-N3 were 5'-TTTCTCGAGCCACCATCATGCCTGGGC-3' (XhoI site underlined) and 5'-TTTGAATTCGAGGCCAGAGCTGGGAAGGC-3' (EcoRI site underlined), respectively. The amplified cDNAs were subjected to nucleotide sequencing using the BigDye terminator cycle sequencing kit (Applied Biosystems, Foster City, CA) and the ABI prism 3100 genetic analyzer (Applied Biosystems). The plasmid for the expression of N-terminally FLAG-tagged mouse Hnrpab in mammalian cells was prepared as described previously [16].

#### 2.4 Cell culture, plasmid transfection, stress induction, and subcellular fractionation

Human embryonic kidney 293T, human cervical carcinoma HeLa, human mammary carcinoma MCF-7, and African green monkey kidney COS-1 were cultured as described previously [17, 18]. Expression vectors were transfected into mammalian cells by using HilyMax (Dojindo, Kumamoto, Japan) or polyethyleneimine (PEI-Max, Polysciences, Warrington, PA) [19]. To observe stress granules, MCF-7 cells were treated with 0.5 mM sodium arsenite for 45 min at 37°C.

For subcellular fractionation, 293T cells were scraped, washed with saline, and lysed with 10 mM Tris-HCl, pH 7.5, containing 1% Triton X-100, 0.15 M NaCl, 1.0 mM EDTA, 1 mM phenylmethanesulfonyl fluoride, 10 µg/ml aprotinin, 1 µg/ml leupeptin, 1 µg/ml pepstatin A, and 50 µM proteasome inhibitor I (Peptide Institute, Osaka, Japan). Supernatant (cytoplasmic fraction) was separated from nuclear precipitates by centrifugation at 10,000 g for 20 min at 4°C. For further fractionation, the cytoplasmic supernatant was ultracentrifuged at 105,000g for 60 min at 4°C, yielding the pellet (P100) and the supernatant (S100). The S100 fraction was mixed with an equal volume of 2 x sample buffer for sodium dodecyl sulfate-polyacrylamide gel electrophoresis (SDS-PAGE) and boiled for 10 min. The nuclear and P100 precipitates were dissolved and boiled in the same volume of 1 x SDS-PAGE sample buffer.

#### 2.5 Antibodies

Rabbit polyclonal anti-human Serbp1 antibody (HPA020559) was obtained from Sigma-Aldrich (St. Louis, MO). According to the supplier's information, this antibody was raised in a recombinant polypeptide including the N-terminal region (residues 3-139) of human Serbp1 (Supplementary Figure S1). The following antibodies were

purchased: mouse monoclonal anti-FLAG antibody (M2) and anti- $\alpha$ -tubulin antibody from Sigma-Aldrich. Rabbit monoclonal antibodies against fibrillarin and ribosomal protein S6 from Cell Signaling Technology (Danvers, MA). Rabbit polyclonal anti-FLAG/DDDDK antibody and anti-GFP antibody from Medical & Biological Laboratories (Nagoya, Japan). Mouse monoclonal antibody (sc-32318) against poly(A)-binding protein 1 (PABP1) [20] and rabbit polyclonal antibody against ribosomal protein L10/QM from Santa Cruz Biotechnology (Santa Cruz, CA). Mouse monoclonal anti-B23/nucleophosmin antibody [21] from Invitrogen. Mouse anti-human G3BP antibody from BD Biosciences (Franklin, NJ).

## 2.6 Immunoblotting and immunofluorescence microscopy

Immunoblotting, including sample preparation, SDS-PAGE, electroblotting, and immunodetection, was described previously [15, 21]. Intensity of protein bands on immunoblots was measured by using the CS analyzer software (Atto, Tokyo, Japan). Immunofluorescence microscopy was performed as described previously [22]. Briefly, cells grown on coverslips were fixed with 2% paraformaldehyde for 15 min and treated with 0.1% Triton X-100 and 1% bovine serum albumin for 30 min. Cells were then incubated with primary antibodies for 1 h and then incubated with fluorophore-conjugated secondary antibodies for 30 min. Nuclei were stained with propidium iodide (Sigma-Aldrich) in some cell samples. The stained cells were examined under a confocal laser-scanning microscope (LSMS Pascal, Carl Zeiss, Oberkochen, Germany). These cells were also observed in differential interference contrast under the same microscope.

## 2.7 Ribosome preparation and analysis

Total cytoplasmic ribosomes were isolated from the rodent testis as described previously [23]. For proteomic analysis of ribosomes, proteins were extracted from isolated ribosomes and subjected to two-dimensional gel electrophoresis [23], which was modified from the radical-free and highly reducing method [24]. After in gel trypsin digestion, protein spots were analyzed by matrix-assisted laser-desorption time-of-flight (TOF) mass spectrometry (MS) and tandem MS (MS/MS), using a 4700 Proteomics Analyzer (Applied Biosystems) and the online Mascot search engine [16, 23].

Total cytoplasmic ribosomes isolated from the rodent testis were subjected to polysome profiling using sucrose gradient sedimentation, as described previously [23]. For polysome profiling by fractionating the cytoplasmic lysate of HeLa cells on a sucrose gradient, the cells were cultured in the presence of 50 µg/ml cycloheximide for 10 min, harvested, washed briefly with saline, and lysed on ice with 20 mM Tris-HCl, pH 7.5, containing 1% Triton X-100, 0.1 M KCl, 5 mM MgCl<sub>2</sub>, 10 mM 2-mercaptoethanol, 1 mM phenylmethanesulfonyl fluoride, 0.5 mg/ml heparin and 10 µg/ml cycloheximide. The lysate was centrifuged twice at 15,000 x g for 10 min at 2°C. The supernatant was layered onto a linear gradient of 15-45% sucrose and ultracentrifuged in a SW41Ti rotor (Beckman, Palo Alto, CA) at 37,000 rpm for 3 h at 2°C. Fraction collection and monitoring (254 nm) were performed as described previously [21]. Ribosomes were dissociated into subunits by treatment of the cell lysate on ice with 25 mM EDTA for 30 min and subjected to the profiling described above.

For limited digestion of ribosomes with ribonuclease (RNase), normally growing MCF-7 cells were pre-treated with cycloheximide, lysed with Triton X-100 and sodium deoxycholate, and ultracentrifuged on sucrose cushion to pellet polysome-rich ribosomes [25]. The purified ribosomes (0.63 absorbance units at 260 nm) were dissolved in a 1.5-ml ultracentrifugation tube (no. S308892A, Hitachi, Tokyo, Japan) which contained 100 µl of 20 mM Tris-HCl, pH 7.5, containing 0.1 M KCl, 5 mM MgCl<sub>2</sub>, 10 mM 2-mercaptoethanol, and 10 µg/ml cycloheximide. The ribosomes were treated with 10 U of Ambion RNase I (AM2294, Thermo Fisher Scientific, Waltham, MA) and incubated for 45 min at 28°C (modified from [26]). The digestion mixture was then placed immediately on ice and ultracentrifuged in an S55A2 rotor (Hitachi) at 100,000g for 1 h at 4°C. The upper part of the supernatant (60 µl) was collected to minimize the contamination of precipitates, mixed with 12 µl of 6 x SDS-PAGE sample buffer, and boiled for 5 min. After careful removal of the remaining supernatant, the pellet was dissolved in 120 µl of 1 x SDS-PAGE sample buffer and boiled. These samples were subjected to immunoblotting.

### 3 RESULTS

#### 3.1 Overexpressed Serbp1 was located in the nucleolus as well as in the cytoplasm, irrespective of isoform

According to the previous study [6] and the Gene site

(<https://www.ncbi.nlm.nih.gov/gene>) of the National Center for Biotechnology Information (NCBI), Serbp1 gene can produce several isoforms by alternative splicing in mammals. For example, Serbp1 genes of mice, rats, and humans have a common exon-intron structure, and four translated isoforms per gene have been indicated (NCBI Gene ID: 66870, 246303, and 26135, respectively). These four isoforms of the two rodent species are depicted in Figure 1A. Human Serbp1 gene can express similar four isoforms (Supplementary Figure S1). Despite this potential complexity, the intracellular localization and functions of the shortest isoform (isoform 4), which was found first, have mainly been investigated [5, 8, 11, 12, 27]. The two regions (residues 203-208 and 233-247) of the longest form, isoform 1, are absent in isoform 4 (Figure 1A and Supplementary Figure S1) and included in the HABP4\_PA1-RBP1 domain, which has been listed as one of the conserved domains by NCBI and a putative mRNA-binding domain [5]. It could be speculated that these insertions would affect the functional properties of isoforms 1-3. Thus, we started to analyze mammalian Serbp1 including the longer isoforms .

To obtain the cDNAs of mouse Serbp1, we have designed PCR with the primers, whose positions are outside the coding region, in principle, to be able to amplify cDNAs encoding all four isoforms in one reaction. Although Serbp1 is ubiquitously expressed in mouse tissues, as suggested by our RT-PCR (Figure 1B) and DNA microarray data (BioGPS (<http://biogps.org/>), ID no. 66870), we used total cDNA obtained from the testis because (i) post-transcriptional control of gene expression is known to be important in this tissue [28] and (ii) we have found novel genes expressing paralogs of ribosomal proteins [15, 22, 23]. We cloned the amplified cDNAs into plasmid vectors for the overexpression of the corresponding proteins bearing a GFP tag in mammalian cells. Nucleotide sequencing showed that the cDNAs encoding full-length isoforms 1 and 3 were obtained.

These expression vectors were then introduced into human 293T cells. Expression of the GFP-fused Serbp1 was confirmed by immunoblotting with anti-GFP antibody (Figure 1C). Fluorescence microscopy showed a dispersed signal in the cytoplasm and bright large spots within nuclei, and no obvious difference in staining pattern was observed between isoforms 1 and 3 (Figure 2A and Supplementary Figure S2A). Biochemical subcellular fractionation also indicated that the distribution of these two isoforms between the cytosol and the nucleus was similar (Supplementary Figure S3). The staining pattern was very similar to that of GFP-fused isoform 4 [27]. The nuclear

spots were indicated to be colocalized with nucleoli by using fibrillarin as a marker (Figure 2B and Supplementary Figure S2B). Some nuclear granules including Serbp1 did not colocalize with nucleoli and might be Cajal bodies according to the previous report on isoform 4 [29]. Although Serbp1 isoform 4 has also been found not only in the cytoplasm but also in the nucleolus [27, 29], the nucleolar localization of this mRNA-binding protein was somewhat puzzling because nuclear mRNA maturation has been reported to occur, for example, in nuclear speckles [30]. Actually, Hnrpab [16], one of the heterogeneous nuclear ribonucleoproteins bound to pre-mRNA [31], was not colocalized with nucleoli, even under overexpression conditions (Figure 2C). Recently, the isoform 4 of Serbp1 has been reported to be included in stress granules [27], which are large cytoplasmic complexes including mRNA binding proteins such as G3BP and appear under oxidative stress conditions, for example in the presence of arsenite [20] (Figure 2D). The isoforms 1 and 3 were also colocalized in stress granules under these conditions (Figure 2E and Supplementary Figure S2C). Overall, the localization in the nucleolus and the cytoplasm is unlikely to be a property of the specific isoform of Serbp1.

### 3.2 Most of cytoplasmic Serbp1 molecules were precipitated by ultracentrifugation

Despite the results described above, there was a possibility that overexpression conditions might affect the intracellular localization of GFP-fused Serbp1. Hence, we tried to visualize endogenous Serbp1 in cultured cells using anti-Serbp1 antibody. This anti-Serbp1 antibody recognizes the N-terminal region of human Serbp1 and is able to bind to all the four isoforms (Supplementary Figure S1). In immunoblotting with anti-Serbp1 antibody, putative endogenous Serbp1 was detected as a single band from three human cell lines and monkey COS-1 cells (Figure 3A). Since differences in molecular mass between the four isoforms of Serbp1 are small (their calculated molecular masses are listed in Supplementary Figure S1), we could not identify the isoform(s) detected by immunoblotting. Serbp1 detected here migrated more slowly than calculated on the gel. The low electrophoretic mobility of this protein (isoform 4) was reported previously [5].

Serbp1 within 293T cells was hardly detected by immunocytochemistry with anti-Serbp1 antibody. Only faint signals were observed in the cytoplasm (Figure 3B, high contrast images because of weak fluorescent signals). To overcome this problem, we analyzed the localization of Serbp1 in 293T cells by biochemical subcellular

fractionation. This analysis (Figure 3C) showed that a portion of endogenous Serbp1 was included in the nuclear fraction, supporting the nuclear localization of this protein indicated in Figure 2. Fractionation of 293T cells overexpressing GFP-fused Serbp1 by the same method showed the similar distributions of overexpressed and endogenous Serbp1 molecules in the nuclear, S100, and P100 fractions (Figure 3D), suggesting that overexpression or the presence of the GFP tag did not obviously disturb the intracellular localization of Serbp1.

Most of cytoplasmic Serbp1 molecules were recovered as precipitates (in the P100 fraction) (Figure 3, C and D). It is very unlikely that free Serbp1 is collected in P100 fraction by ultracentrifugation. This finding suggests that many of cytoplasmic Serbp1 molecules are included in large complexes.

### 3.3 Proteomic analysis identified Serbp1 in the cytoplasmic ribosomes of the rodent testis

Subcellular fractionation indicated most of cytoplasmic Serbp1 molecules in the P100 fraction. Because the cells were lysed with the detergent Triton X-100, membrane-enclosed organelles such as microsomes were not included in the P100 fraction. Actually under a fluorescence microscope, no membranous structures were observed in the cytoplasm of the cell expressing GFP-fused Serbp1 (Figure 2A and Supplementary Figure S2A). Although Serbp1 has been observed in stress granules under oxidative stress conditions [27] (Figure 2E and Supplementary Figure S2C), these granules were hardly visible in cells under normal growth conditions [27] (Figure 2D). Microscopy in this study also indicated the presence of Serbp1 in nucleoli (Figure 2B). It has long been recognized that the nucleolus is a place where RNA polymerase I resides and ribosome biogenesis occurs [32], although other additional functions have recently been reported [33]. Serbp1 knockdown exhibited a defect in nucleolar pre-ribosomal RNA processing in HeLa cells [34]. In addition, direct associations of Serbp1 with ribosomal proteins have been shown in previous proteomic studies (see the Discussion of [27]). Cytoplasmic ribosomes, including polysomes, the 80S ribosome (monosome), and the small (40S) and large (60S) subunits, are precipitated by ultracentrifugation [21, 35]. Hence, we asked whether Serbp1 was included in cytoplasmic ribosomes.

Previously, we have developed a proteomic analysis system of mammalian ribosomes,

which is a combination of two-dimensional electrophoresis suitable for the separation of mammalian ribosomal proteins, including small hyper-basic ones, in-gel tryptic digestion, and MS, and identified 78 known ribosomal proteins from the ribosomes of rodent tissues including the testis [23]. After the protein constituents of rat testis ribosomes were separated (Figure 4A), we examined the spots other than those of the known ribosomal proteins on the gels and found Serbp1 by TOF-MS (Figure 4B, Table 1, and Supplementary Table S1) and MS/MS (Figure 4C and Table 1). One of the identified peptide by TOF-MS included the amino acid residues absent in isoforms 3 and 4 (underlined in Table 1) although the Mascot score for Serbp1 by TOF-MS was low (71). These MS data suggested the association of Serbp1 with ribosomes in the cytoplasm.

#### 3.4 Serbp1 was associated with the small 40S subunit and included in polysomes in normal and cancer cells

To further delineate the localization of Serbp1 in rodent cytoplasmic ribosomes, Serbp1 was analyzed by polysome profiling including density gradient-velocity sedimentation.

The peptide sequence of human Serbp1 used as the immunogen of the anti-human Serbp1 antibody is 97% identical to the corresponding sequence of mouse Serbp1 (Figure 1A). Mouse Serbp1 overexpressed in 293T cells was clearly detected by immunoblotting with anti-human Serbp1 antibody (Figure 5A), confirming cross-reactivity of the antibody to mouse Serbp1. Serbp1 was indicated to be detected specifically in immunoblotting of the cytoplasmic lysate of the mouse testis (Figure 5B). After these confirmations, cytoplasmic ribosomes were isolated from the mouse testis and subjected to sucrose linear gradient ultracentrifugation. Ribosomes and their subunits were separated basically according to their molecular mass (Figure 5C). Serbp1 was suggested to be a component of the small 40S subunit because the protein was co-sedimented with this subunit. In addition, Serbp1 was detected in the fractions including polysomes, suggesting the inclusion of Serbp1 in actively translating ribosomes.

Serbp1 was expressed in normal tissues (Figure 1B) and cancer cells (Figure 3A). Potential importance of Serbp1 in tumor progression has been reported [36-39]. High-resolution of cryo-electron microscopy of the 80S ribosome of human peripheral blood mononuclear cells has shown the presence of Serbp1 in the 40S subunit [40].

However, Serbp1 was not identified in the 80S ribosome of HeLa cells by using the same microscopic method [41] (although recent cross-linking MS has indicated the interaction between this protein and the 40S subunit in HeLa cells [42]). One possibility was that Serbp1 would be associated with the ribosome depending on the intracellular environment and mainly play other roles (described in the Introduction section) in cancer cells. These stimulated us to investigate whether Serbp1 was included in ribosomes in cancer cells.

The cytoplasmic lysates were prepared from HeLa cells (Figure 3A) and subjected to polysome profiling. Serbp1 was detected in the fractions including the 40S subunit, the 80S ribosome, and polysomes (Figure 6A). Serbp1 was detected also in the fractions including the particles smaller than the 40S subunit. This might reflect the fact that Serbp1 functions interacting with various proteins [7, 9, 10, 13]. To examine whether Serbp1 was associated with unknown heavy complexes or aggregates and therefore co-sedimented with polysomes, the cell lysate was pre-treated with EDTA and subjected to polysome profiling. EDTA irreversibly dissociates the 80S ribosome into the 40S and 60S subunits, and mRNAs are released from polysomes [43, 44]. Most polysomes disappeared and the amount of the two subunits increased after EDTA treatment (Figure 6B). Ribosomal proteins and Serbp1 in heavy fractions were scarcely visible by immunoblotting. The substantial amount of Serbp1 was still detected in the fractions including the 40S subunit after subunit dissociation, suggesting association of this protein with the subunit itself. Although we cannot completely exclude the possibility that mRNA-protein (messenger ribonucleoprotein) complexes containing Serbp1 were released from polysomes by EDTA and sedimented in the fractions including the 40S subunit in the ultracentrifugation, it has been reported that mRNA-protein complexes have a heterogeneous sedimentation profile (sedimentation coefficient, 20S to greater than 100S) under these experimental conditions [44] and that most of them sediment faster than the large 60S subunit [45]. Figure 6B also shows a portion of ribosomal protein S6 in the fractions including particles heavier than the 40S subunit. Although the precise nature of the particles including S6 is unclear, since ribosomal protein L10 was also detected in these fractions, the two subunits of some monosomes and oligosomes might remain associated under the conditions of the EDTA treatment. Or, unknown, artificial aggregates including ribosomal components might be formed during the irreversible subunit inactivation by EDTA [43, 46]. Despite this ambiguity, the altered sedimentation profile of Serbp1 was clearly observed by the EDTA treatment, supporting Serbp1 as an auxiliary protein associated with cytoplasmic ribosomes.

Finally, limited RNase digestion of ribosomes purified from cancer cells was performed to examine the association of Serbp1 with polysomes. The digestion conditions are based on those used in translation complex profile sequencing (TCP-seq) [26]. The limited digestion causes cleavage of the mRNA regions that are not protected by translating ribosomes. Serbp1 has been reported to bind to the untranslated regions of target mRNAs [6, 12, 47]. Given that the association of Serbp1 with polysomes was mediated by its interaction with mRNA, some, if not all, of Serbp1 molecules were considered to be released from ribosomes after the digestion. Released mRNA-binding proteins and RNase-resistant ribosomes were separated by ultracentrifugation and observed by immunoblotting (Figure 6C). Ribosomal proteins S6 and L10 were detected in ribosomes collected as the pellet. The amounts of PABP and G3BP/RBP42, which are mRNA-binding proteins and interact with polysomes in an mRNA-dependent manner [48], increased in the supernatant after the RNase digestion. Serbp1 in the supernatant was hardly visible after the digestion, suggesting that the association is mRNA-independent.

#### 4 DISCUSSION

Whereas the primary function of the cytoplasmic ribosome is to decode mRNA into polypeptides, accumulating data indicate that ribosomes themselves regulate gene expression, including translation of a select group of mRNAs [49, 50]. As one of the mechanisms to achieve such selective translation, a part of the components, including accessory proteins, of ribosomes in the cell are supposed to change according to growth and developmental cues, meaning the heterogeneity of ribosomes or specialized ribosomes [51, 52]. Dysfunction or deregulation of ribosomes has been proposed to cause aberrant translation, resulting in diseases including cancer [53, 54]. Therefore, analyses of the composition and chemical modifications of the protein constituents of ribosomes under various physiological and pathological conditions have been anticipated to reveal another layer of complexity in gene regulation [23, 55, 56].

We analyzed mammalian Serbp1, which was suggested to be associated with ribosomes, as a component of the small 40S subunit, in normal testis (Figures 4 and 5) and cancer cells including HeLa cells (Figure 6). In the previous cryo-electron microscopy of the 80S ribosome of HeLa cells, Serbp1 was not identified [41]. This might be related to the following two points. (i) Serbp1 is assumed to be a sub-stoichiometric component of the

ribosome (see also Figure 4A), probably to regulate translation of a subset of mRNAs. (ii) The 80S ribosome was prepared from confluent HeLa cells after 6-h serum starvation [57]. Though this pre-treatment is certainly reasonable to synchronize cell population and to obtain the homogeneous ribosome, it seems possible that the growth-restricting conditions influence the association of translation-regulating factors with ribosomes. Serbp1 and its yeast homologue Stm1 have been reported to be involved in translational regulation, which includes their interaction with the 40S subunits [47, 58-61]. However, the molecular mechanisms underlying the regulation have not been fully clarified. In view of the multifaceted properties of Serbp1 (see the Introduction), careful molecular dissection of Serbp1 is apparently important to distinguish the effect on gene expression caused by the ribosome-binding activity of Serbp1 from that caused by other activities of this protein. For example, after identification of the region of Serbp1 that is specifically needed for association with the 40S subunit, the effect of Serbp1 mutants defective in ribosome binding on translation would be able to be investigated in vitro. Based on these considerations, we tried to set up an in vitro translation assay[35] including rabbit reticulocyte lysates and recombinant proteins produced in bacteria, which has unfortunately been unsuccessful since full-length recombinant Serbp1 became insoluble in bacterial cells (our unpublished results).

In summary, our findings provide a new insight into the mechanisms underlying the post-transcriptional gene regulation by Serbp1. Further mechanistic studies are expected for a deeper understanding of tumor malignancy, in addition to translational control, considering an emerging link between Serbp1 and tumor progression [36-39].

#### ACKNOWLEDGEMENTS

We thank Dr. Yuki Taga and Ryo Kojima (Nagoya University) for technical supports and helpful discussions. This work was supported in part by JSPS KAKENHI (25450514 and 17K07751).

#### CONFLICT OF INTEREST

The authors declare no conflict of interest.

#### REFERENCES

1. Pennisi E. Shining a light on the genome's 'dark matter'. *Science* 2010;330:1614.
2. Nilsen TW, Graveley BR. Expansion of the eukaryotic proteome by alternative splicing. *Nature* 2010;463:457-463.
3. Gerstberger S, Hafner M, Tuschl T. A census of human RNA-binding proteins. *Nat Rev Genet* 2014;15:829-845.
4. Glisovic T, Bachorik JL, Yong J, Dreyfuss G. RNA-binding proteins and post-transcriptional gene regulation. *FEBS Lett* 2008;582:1977-1986.
5. Heaton JH, Dlakic WM, Dlakic M, Gelehrter TD. Identification and cDNA cloning of a novel RNA-binding protein that interacts with the cyclic nucleotide-responsive sequence in the type-1 plasminogen activator inhibitor mRNA. *J Biol Chem* 2001;276:3341-3347.
6. Heaton JH, Dlakic WM, Gelehrter TD. Posttranscriptional regulation of PAI-1 gene expression. *Thromb Haemost* 2003;89:959-966.
7. Mondal S, Begum NA, Hu WJ, Honjo T. Functional requirements of AID's higher order structures and their interaction with RNA-binding proteins. *Proc Natl Acad Sci USA* 2016;113:E1545-E1554.
8. Lemos TA, Passos DO, Nery FC, Kobarg J. Characterization of a new family of proteins that interact with the C-terminal region of the chromatin-remodeling factor CHD-3(1). *FEBS Lett* 2003;533:14-20.
9. Mari Y, West GM, Scharager-Tapia C, Pascal BD, Garcia-Ordenez RD, Griffin PR. SERBP1 is a component of the liver receptor homologue-1 transcriptional complex. *J Proteome Res* 2015;14:4571-4580.
10. Fernandes MS, Brosens JJ, Gellersen B. Honey, we need to talk about the membrane progesterin receptors. *Steroids* 2008;73:942-952.
11. Lee YJ, Hsieh WY, Chen LY, Li C. Protein arginine methylation of SERBP1 by protein arginine methyltransferase 1 affects cytoplasmic/nuclear distribution. *J Cell Biochem* 2012;113:2721-2728.
12. Ahn JW, Kim S, Na W, Baek SJ, Kim JH, Min K, Yeom J, Kwak H, Jeong S, Lee C, Kim SY, Choi CY. SERBP1 affects homologous recombination-mediated DNA repair by regulation of CtIP translation during S phase. *Nucleic Acids Res* 2015;43:6321-6333.
13. Chew TG, Peaston A, Lim AK, Lorthongpanich C, Knowles BB, Solter D. A tudor domain protein SPINDLIN1 interacts with the mRNA-binding protein SERBP1 and is involved in mouse oocyte meiotic resumption. *Plos One* 2013;8:e69764.

14. Nakamura M, Tomita A, Nakatani H, Matsuda T, Nadano D. Antioxidant and antibacterial genes are upregulated in early involution of the mouse mammary gland: sharp increase of ceruloplasmin and lactoferrin in accumulating breast milk. *DNA Cell Biol* 2006;25:491-500.
15. Sugihara Y, Sadohara E, Yonezawa K, Kugo M, Oshima K, Matsuda T, Nadano D. Identification and expression of an autosomal paralogue of ribosomal protein S4, X-linked, in mice: Potential involvement of testis-specific ribosomal proteins in translation and spermatogenesis. *Gene* 2013;521:91-99.
16. Taga Y, Miyoshi M, Okajima T, Matsuda T, Nadano D. Identification of heterogeneous nuclear ribonucleoprotein A/B as a cytoplasmic mRNA-binding protein in early involution of the mouse mammary gland. *Cell Biochem Funct* 2010;28:321-328.
17. Nadano D, Aoki C, Yoshinaka T, Irie S, Sato T. Electrophoretic characterization of ribosomal subunits and proteins in apoptosis: specific down-regulation of S11 in staurosporine-treated human breast carcinoma cells. *Biochemistry* 2001;40:15184-15193.
18. Nadano D, Nakayama J, Matsuzawa S, Sato T, Matsuda T, Fukuda MN. Human tasin, a proline-rich cytoplasmic protein, associates with the microtubular cytoskeleton. *Biochem J* 2002;364:669-677.
19. Thomas M, Lu JJ, Ge Q, Zhang CC, Chen JZ, Klivanov AM. Full deacylation of polyethylenimine dramatically boosts its gene delivery efficiency and specificity to mouse lung. *Proc Natl Acad Sci USA* 2005;102:5679-5684.
20. Kedersha N, Anderson P. Mammalian stress granules and processing bodies. *Methods Enzymol* 2007;431:61-81.
21. Miyoshi M, Okajima T, Matsuda T, Fukuda MN, Nadano D. Bystin in human cancer cells: intracellular localization and function in ribosome biogenesis. *Biochem J* 2007;404:373-381.
22. Nadano D, Notsu T, Matsuda T, Sato T. A human gene encoding a protein homologous to ribosomal protein L39 is normally expressed in the testis and derepressed in multiple cancer cells. *Biochim Biophys Acta* 2002;1577:430-436.
23. Sugihara Y, Honda H, Iida T, Morinaga T, Hino S, Okajima T, Matsuda T, Nadano D. Proteomic analysis of rodent ribosomes revealed heterogeneity including ribosomal proteins L10-like, L22-like 1, and L39-like. *J Proteome Res* 2010;9:1351-1366.
24. Wada A. Analysis of *Escherichia coli* ribosomal proteins by an improved two dimensional gel electrophoresis. Detection of four new proteins. *J Biochem*

- 1986;100:1583-1594.
25. Nadano D, Ishihara G, Aoki C, Yoshinaka T, Irie S, Sato T. Preparation and characterization of antibodies against human ribosomal proteins: heterogeneous expression of S11 and S30 in a panel of human cancer cell lines. *Jpn J Cancer Res* 2000;91:802-810.
  26. Shirokikh NE, Archer SK, Beilharz TH, Powell D, Preiss T. Translation complex profile sequencing to study the in vivo dynamics of mRNA- ribosome interactions during translation initiation, elongation and termination. *Nat Protoc* 2017;12:697-731.
  27. Lee YJ, Wei HM, Chen LY, Li C. Localization of SERBP1 in stress granules and nucleoli. *FEBS J* 2014;281:352-364.
  28. Kleene KC. Patterns, mechanisms, and functions of translation regulation in mammalian spermatogenic cells. *Cytogenet. Genome Res* 2003;103:217-224.
  29. Lemos TA, Kobarg J. CGI-55 interacts with nuclear proteins and co-localizes to p80-coilin positive-coiled bodies in the nucleus. *Cell Biochem Biophys* 2006;44:463-474.
  30. Mao YTS, Zhang B, Spector DL. Biogenesis and function of nuclear bodies. *Trends Genet* 2011;27:295-306.
  31. Geuens T, Bouhy D, Timmerman V. The hnRNP family: insights into their role in health and disease. *Hum Genet* 2016;135:851-867.
  32. Takahashi N, Yanagida M, Fujiyama S, Hayano T, Isobe T. Proteomic snapshot analyses of preribosomal ribonucleoprotein complexes formed at various stages of ribosome biogenesis in yeast and mammalian cells. *Mass Spectrom Rev* 2003;22:287-317.
  33. Boisvert FM, van Koningsbruggen S, Navascues J, Lamond AI. The multifunctional nucleolus. *Nat Rev Mol Cell Biol* 2007;8:574-585.
  34. Tafforeau L, Zorbas C, Langhendries JL, Mullineux ST, Stamatopoulou V, Mullier R, Wacheu L, Lafontaine DLJ. The Complexity of human ribosome biogenesis revealed by systematic nucleolar screening of pre-rRNA processing factors. *Mol Cell* 2013;51:539-551.
  35. Yonezawa K, Sugihara Y, Oshima K, Matsuda T, Nadano D. Lyar, a cell growth-regulating zinc finger protein, was identified to be associated with cytoplasmic ribosomes in male germ and cancer cells. *Mol Cell Biochem.* 2014;395:221-229.
  36. Koensgen D, Mustea A, Klaman I, Sun P, Zafrakas M, Lichtenegger W, Denkert C, Dahl E, Sehouli J. Expression analysis and RNA localization of PAI-RBP1

- (SERBP1) in epithelial ovarian cancer: Association with tumor progression. *Gynecol Oncol.* 2007;107:266-273.
37. Kunkle BW, Yoo C, Roy D. Reverse engineering of modified genes by Bayesian network analysis defines molecular determinants critical to the development of glioblastoma. *Plos One* 2013;8:e64140.
  38. Serce NB, Boesl A, Klaman I, von Serenyi S, Noetzel E, Press MF, Dimmler A, Hartmann A, Sehouli J, Knuechel R, Beckmann MW, Fasching PA, et al. Overexpression of SERBP1 (Plasminogen activator inhibitor 1 RNA binding protein) in human breast cancer is correlated with favourable prognosis. *BMC Cancer* 2012;12:597.
  39. Wolfer A, Wittner BS, Irimia D, Flavin RJ, Lupien M, Gunawardane RN, Meyer CA, Lightcap ES, Tamayo P, Mesirov JP, Liu XS, Shioda T, et al. MYC regulation of a "poor-prognosis" metastatic cancer cell state. *Proc Natl Acad Sci USA* 2010;107:3698-3703.
  40. Anger AM, Armache JP, Berninghausen O, Habeck M, Subklewe M, Wilson DN, Beckmann R. Structures of the human and Drosophila 80S ribosome. *Nature* 2013;497:80-85.
  41. Khatter H, Myasnikov AG, Natchiar SK, Klaholz BP. Structure of the human 80S ribosome. *Nature* 2015;520:640-645.
  42. Liu F, Rijkers DTS, Post H, Heck AJR. Proteome-wide profiling of protein assemblies by cross-linking mass spectrometry. *Nat Methods* 2015;12:1179-1184.
  43. Tashiro Y, Morimoto T. Sedimentation studies on the interaction of ribosomal subunits from liver. *Biochim Biophys Acta* 1966;123:523-533.
  44. Henshaw EC. Messenger RNA in rat liver polyribosomes: evidence that it exists as ribonucleoprotein particles. *J Mol Biol* 1968;36:401-411.
  45. Kumar A, Lindberg U. Characterization of messenger ribonucleoprotein and messenger RNA from KB cells. *Proc Natl Acad Sci USA* 1972;69:681-685.
  46. Terao K, Takahashi Y, Ogata K. Differences between the protein moieties of active subunits and EDTA-treated subunits of rat liver ribosomes with specific references to a 5 S rRNA · protein complex. *Biochim Biophys Acta* 1975;402:230-237.
  47. Lu H, Li WQ, Noble WS, Payan D, Anderson DC. Riboproteomics of the hepatitis C virus internal ribosomal entry site. *J Proteome Res* 2004;3:949-957.
  48. Das A, Morales R, Banday M, Garcia S, Hao L, Cross GAM, Estevez AM, Bellofatto V. The essential polysome-associated RNA-binding protein RBP42

- targets mRNAs involved in *Trypanosoma brucei* energy metabolism. *RNA* 2012;18:1968-1983.
49. Gupta V, Warner JR. Ribosome-omics of the human ribosome. *RNA* 2014;20:1004-1013.
  50. Mauro VP, Matsuda D. Translation regulation by ribosomes: Increased complexity and expanded scope. *RNA Biol.* 2016;13:748-755.
  51. Sauert M, Temmel H, Moll I. Heterogeneity of the translational machinery: Variations on a common theme. *Biochimie* 2015;114:39-47.
  52. Shi Z, Barna M. Translating the genome in time and space: specialized ribosomes, RNA regulons, and RNA-binding proteins. *Ann Rev Cell Dev Biol* 2015;31:31-54.
  53. Narla A, Ebert BL. Ribosomopathies: human disorders of ribosome dysfunction. *Blood* 2010;115:3196-3205.
  54. Stumpf CR, Ruggero D. The cancerous translation apparatus. *Curr Opin Genet Dev* 2011;21:474-483.
  55. Nguyen-Lefebvre AT, Gonin-Giraud S, Scherl A, Arboit P, Granger L, Sanchez JC, Diaz JJ, Gandrillon O, Madjar JJ. Identification of human, rat and chicken ribosomal proteins by a combination of two-dimensional polyacrylamide gel electrophoresis and mass spectrometry. *J Proteomics* 2011;74:167-185.
  56. Reschke M, Clohessy JG, Seitzer N, Goldstein DP, Breitkopf SB, Schmolze DB, Ala U, Asara JM, Beck AH, Pandolfi PP. Characterization and analysis of the composition and dynamics of the mammalian riboproteome. *Cell Rep* 2013;4:1276-1287.
  57. Khatteer H, Myasnikov AG, Mastio L, Billas IML, Birck C, Stella S, Klaholz BP. Purification, characterization and crystallization of the human 80S ribosome. *Nucleic Acids Res* 2014;42:e49.
  58. Ben-Shem A, de Loubresse NG, Melnikov S, Jenner L, Yusupova G, Yusupov M. The Structure of the Eukaryotic Ribosome at 3.0 angstrom Resolution. *Science* 2011;334:1524-1529.
  59. Balagopal V, Parker R. Stm1 modulates translation after 80S formation in *Saccharomyces cerevisiae*. *RNA* 2011;17:835-842.
  60. van den Elzen AMG, Schuller A, Green R, Seraphin B. Dom34-Hbs1 mediated dissociation of inactive 80S ribosomes promotes restart of translation after stress. *EMBO J* 2014;33:265-276.
  61. Zinoviev A, Hellen CUT, Pestova TV. Multiple Mechanisms of Reinitiation on Bicistronic Calicivirus mRNAs. *Mol Cell* 2015;57:1059-1073.

## Legends to Figures

Figure 1. Structures and expression of rodent Serbp1. (A) Schematic representation of the four isoforms of mouse/rat Serbp1. The black boxes indicate the HABP4\_PA1-RBP1 domain. “Ab” indicates the region corresponding to that of human Serbp1, which was used as the immunogen for anti-human Serbp1 antibody. Calculated molecular mass of each isoform is indicated on the right. Each isoform of mouse Serbp1 and its rat counterpart have the same amino acid sequence except for three residue differences (asterisks). Owing to alternative splicing of mRNA precursors, the region of residues 203-208 in isoform 1 is absent in isoforms 2 and 4, and the region of residues 233-247 in isoform 1 is absent in isoforms 3 and 4 (these two regions are not drawn to scale). (B) Expression of Serbp1 in normal mouse tissues was analyzed by RT-PCR. (C) Expression of the GFP-fused isoforms of mouse Serbp1 was detected by immunoblotting with anti-GFP antibody. N-terminally GFP-fused isoforms 1 and 3 (GFP-Serbp1-iso1 and GFP-Serbp1-iso3, respectively) and C-terminally GFP-fused isoforms 1 and 3 (Serbp1-iso1-GFP and Serbp1-iso3-GFP, respectively) were expressed in 293T cells, and the whole cell lysates were analyzed.

Figure 2. Intracellular localization of the N-terminally GFP-fused isoforms 1 and 3 of mouse Serbp1. (A) Co-staining of each isoform and nuclei. Human 293T cells expressing GFP were used as a control. Nuclei were stained with propidium iodide (PI). (B) Co-staining of each isoform and a nucleolar marker, fibrillarlin. (C) Co-staining of FLAG-tagged Hnrpab and B23 localized in the nucleolus and the cytoplasm. (D) MCF-7 cells were treated with or without arsenite and stained with a stress granule marker, G3BP. (E) Co-localization of each isoform with stress granules. Cells expressing each isoform or GFP were treated with arsenite before immunofluorescence microscopy. The asterisks indicate nuclei. Scale bars, 10  $\mu$ m. The observation of the C-terminally GFP-fused isoforms 1 and 3 of mouse Serbp1 is shown in Supplementary Figure S2.

Figure 3. Subcellular fractionation indicated endogenous Serbp1 in the P100 fraction. (A) Endogenous Serbp1 and  $\alpha$ -tubulin (control) were detected by immunoblotting. The whole lysates of the four cell lines were analyzed. (B) Immunostaining of Serbp1 in 293T cells with anti-Serbp1 antibody. Normal rabbit IgG was used as a negative control. The images of the same cells in differential interference contrast (DIC) are also shown. Scale bar, 10  $\mu$ m. (C and D) Subcellular fractionation of 293T cells (no transfection) (C)

and 293T cells transiently transfected with the expression vector for the N-terminally GFP-fused isoform 1 of mouse Serbp1 (GFP-Serbp1) (D). After lysis with Triton X-100, 293T cells were centrifuged to collect nuclei. The supernatant was subjected to ultracentrifugation, obtaining the precipitate (P100) and the supernatant (S100). These fractions were subjected to immunoblotting. Fibrillarin, ribosomal protein S6, and  $\alpha$ -tubulin were used as markers for nuclei, P100, and S100, respectively.

Figure 4. Proteomic identification of Serbp1 in rodent testis ribosomes. (A) Two-dimensional protein gel electrophoresis of rat testis ribosomes. Proteins in total cytoplasmic ribosomes were separated by the modified radical-free and highly reducing method and visualized with Coomassie brilliant blue. Partial electrophoretogram is shown. After in-gel tryptic digestion, Serbp1 was detected by MS from the spot indicated by the arrow. Many spots on the right part of the gel are those including known ribosomal proteins. (B) The TOF spectrum of Serbp1 from the spot indicated by the arrow in (A). The m/z peaks in this spectrum correspond to singly charged peptides ( $MH^+$ ). Peak intensity is expressed as percent of the highest peak (peak 5). Data of the numbered peaks were used for protein identification (Table 1 and Supplementary Table S1). (C) MS/MS spectrum of the peak 1 (m/z, 1684.9218) in (B). Thirteen out of 76 fragment ions were matched using 16 most intense peaks.

Figure 5. Serbp1 in testis ribosomes. (A) Cross-reactivity of anti-human Serbp1 antibody with mouse Serbp1. The same samples as used in Figure 1C were subjected to immunoblotting with the antibody. The asterisk indicates endogenous Serbp1 in human 293T cells. (B) Immunoblotting of the cytoplasmic lysate of the mouse testis with anti-Serbp1 antibody. (C) Polysome profiling. Ribosomes were purified from the mouse testis and fractionated by sucrose gradient ultracentrifugation. Fractions were immunoblotted using the antibodies indicated on the left. Ribosomal proteins S6 and L10 were used as markers of the 40S and 60S subunits, respectively.

Figure 6. Identification of Serbp1 in the ribosomes of cancer cells. (A and B) The cytoplasmic lysates of HeLa cells were subjected to sucrose gradient ultracentrifugation and immunoblotted as described in Figure 5C. In (B), the lysate was pre-treated with EDTA before ultracentrifugation. (C) Ribosomes purified from MCF-7 cells were treated with limited amounts of RNase I and ultracentrifuged to yield supernatant (S) and pellet (P). These fractions were subjected to immunoblotting with antibodies against the proteins indicated on the left.

## SIGNIFICANCE OF THE STUDY

In mammalian cells, the final protein output of their genetic program is determined not only by controlling transcription but also by regulating the post-transcriptional events. Although mRNA-binding proteins and the cytoplasmic ribosome have long been recognized as central players in the post-transcriptional regulation, their physical and functional interactions are still far from a complete understanding. Here, we describe the intracellular localization of Serbp1, an mRNA-binding protein, and the inclusion of this protein in actively translating ribosomes in normal and cancer cells. These findings shed a new light into molecular mechanisms underlying Serbp1 action in translational gene regulation and tumor progression.

Table 1. Identification by MS from the spot indicated by the arrow in Figure 4A

Protein	Accession number	Identification method	Score	Identified peptide <sup>a</sup>		Peak no. in Figure 4B
				Residue #	Sequence	
Serbp1 <sup>b</sup>	XP_006236678.1	PMF <sup>c</sup>	71	2 – 16	PGHLQEGFGCVVTNR	1
				17 – 32	FDQLFDDESDPFEVLK	2
				112 – 122	RPDQQLQGDGK	3
				137 – 145	RFEKPLEEK	4
				217 – 236	GGSGSHNWGTVKDEL <u>TESPK</u> <sup>d</sup>	5
				327 – 344	SKSEEAHAEDSVMDHHFR	6
				327 – 344	SKSEEAHAEDSVMDHHFR (including M oxidization)	7
				329 – 344	SEEAHAEDSVMDHHFR	8
				329 – 344	SEEAHAEDSVMDHHFR (including M oxidization)	9
		MS/MS	70	2 – 16	PGHLQEGFGCVVTNR <sup>e</sup>	
			52	17 – 32	FDQLFDDESDPFEVLK	

<sup>a</sup> One missed cleavage was allowed in a Mascot search.

<sup>b</sup> The isoforms 1 and 2 of rat Serbp1 were listed as significant candidates. The results on isoform 1 are shown here.

<sup>c</sup> TOF spectrum is shown in Figure 4B. Details of the TOF-MS data are listed in Supplementary Table S1. PMF, peptide mass fingerprinting.

<sup>d</sup> The underlined residues are not included in the isoforms 3 or 4 of rat Serbp1 (Figure 1A).

<sup>e</sup> MS/MS spectrum of this fragment is shown in Figure 4C.

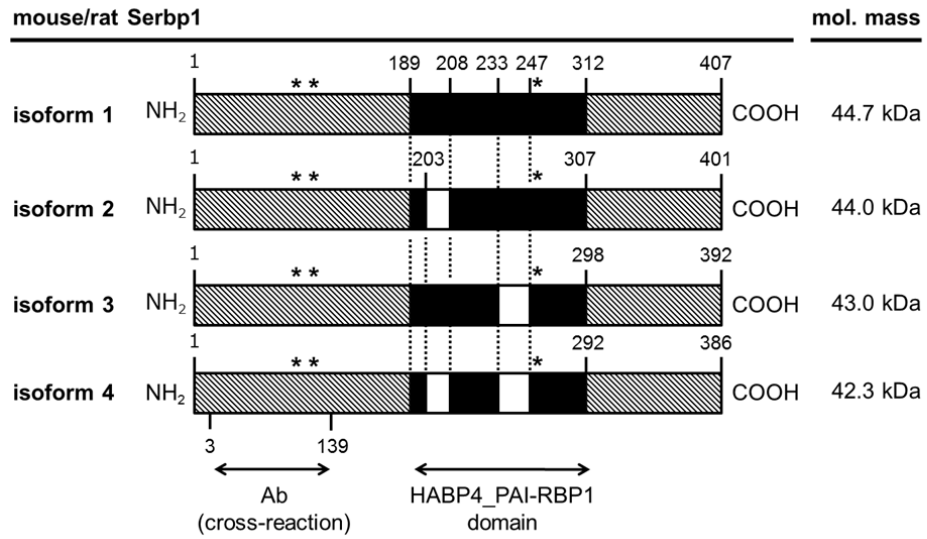
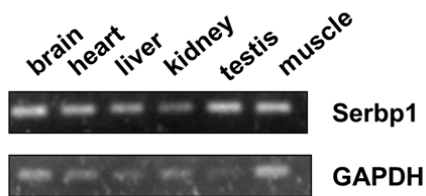
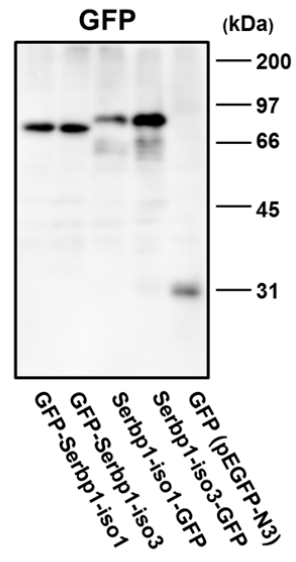
**A****B****C**

Figure 1

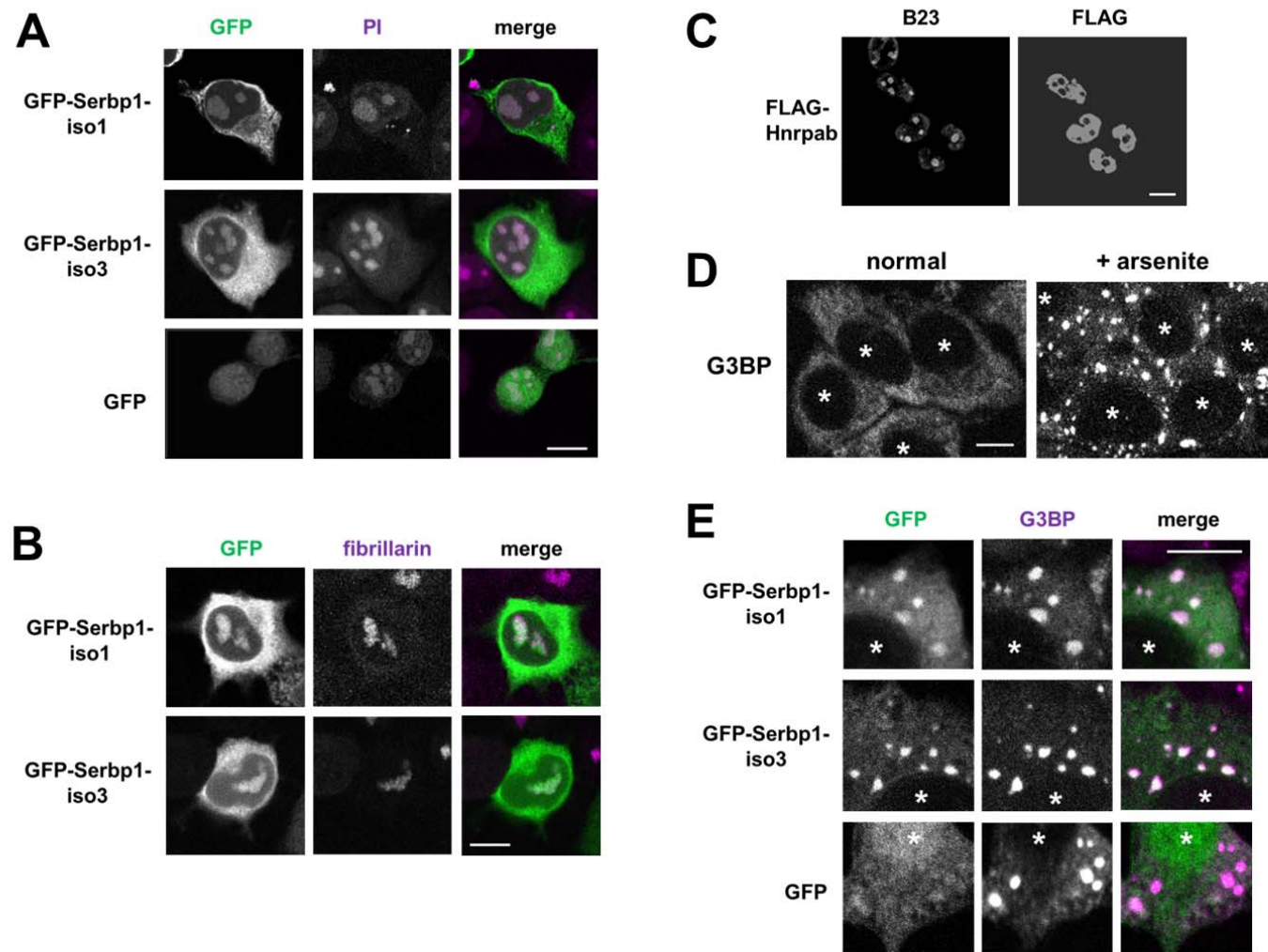


Figure 2

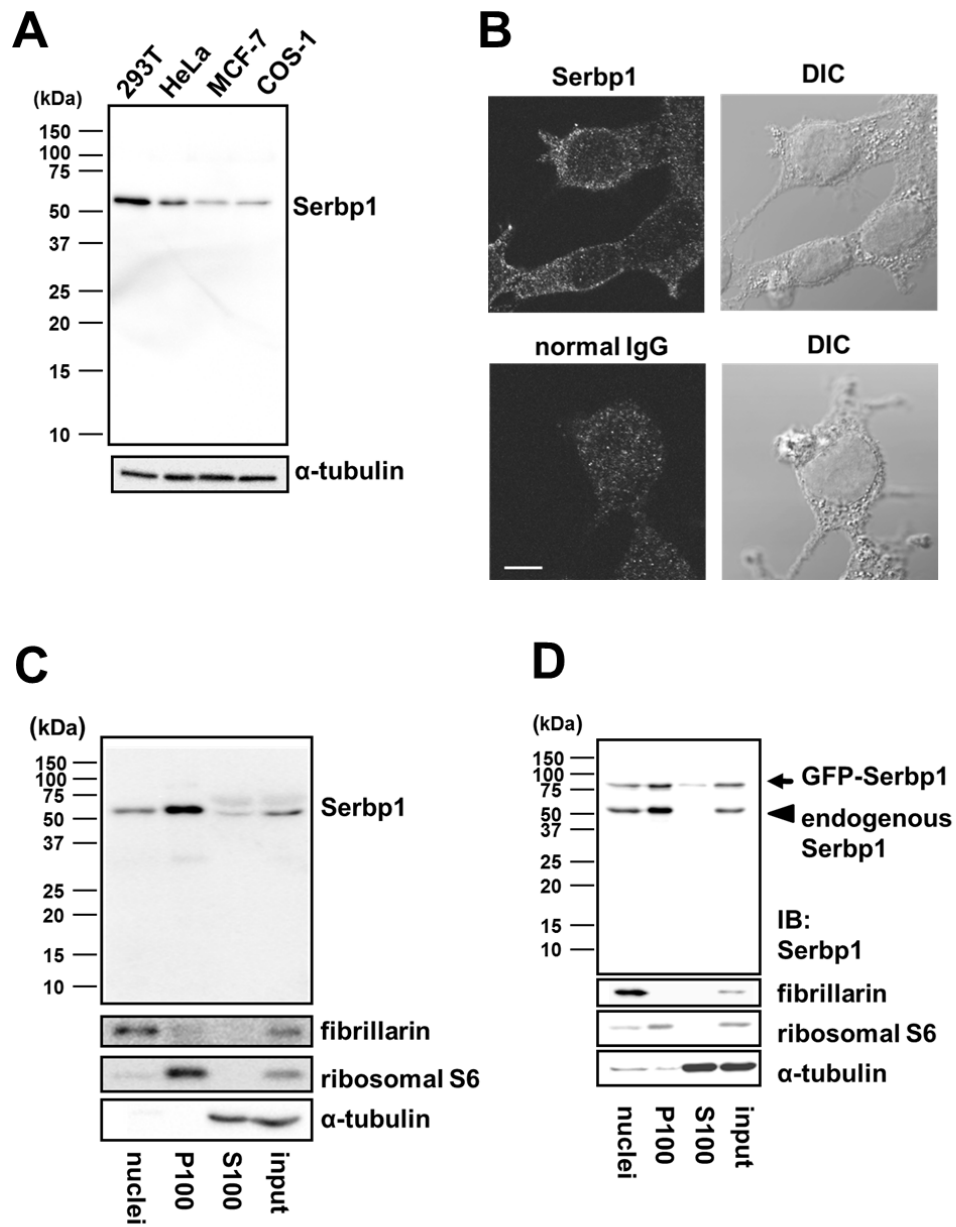


Figure 3





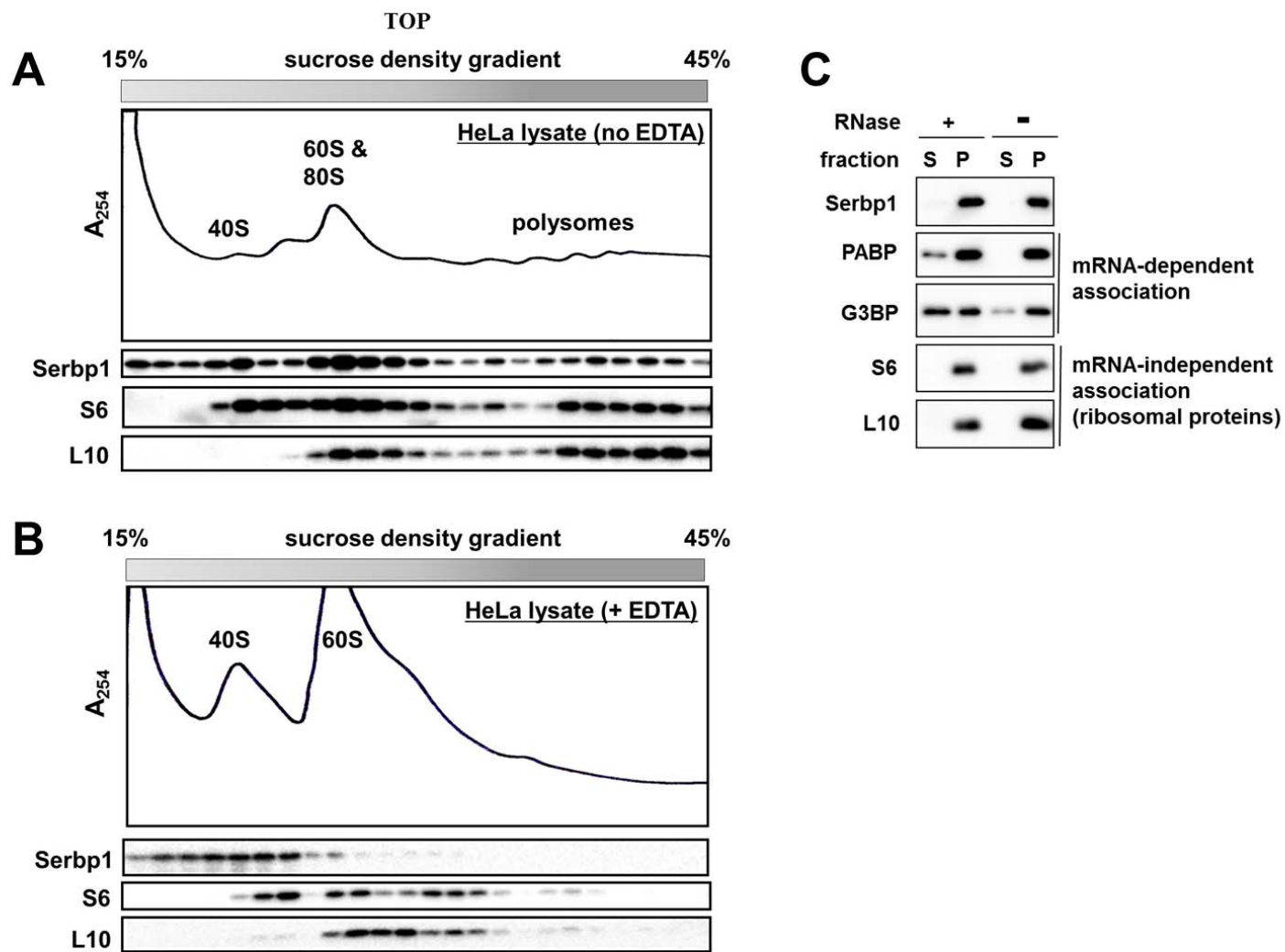
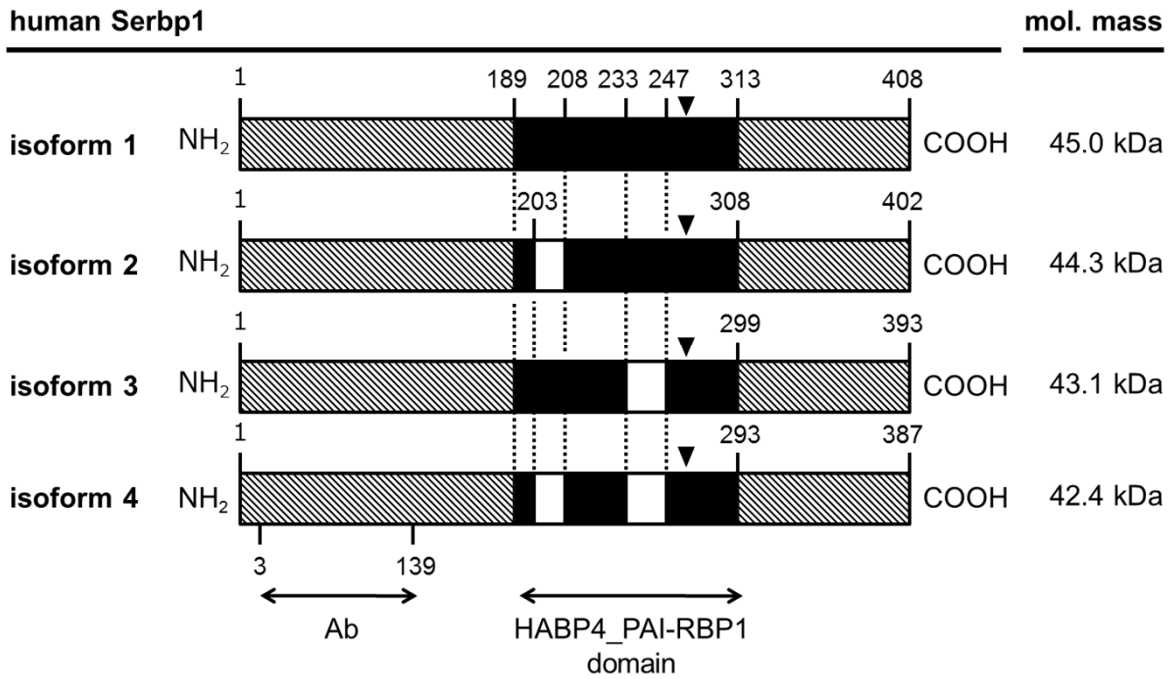


Figure 6

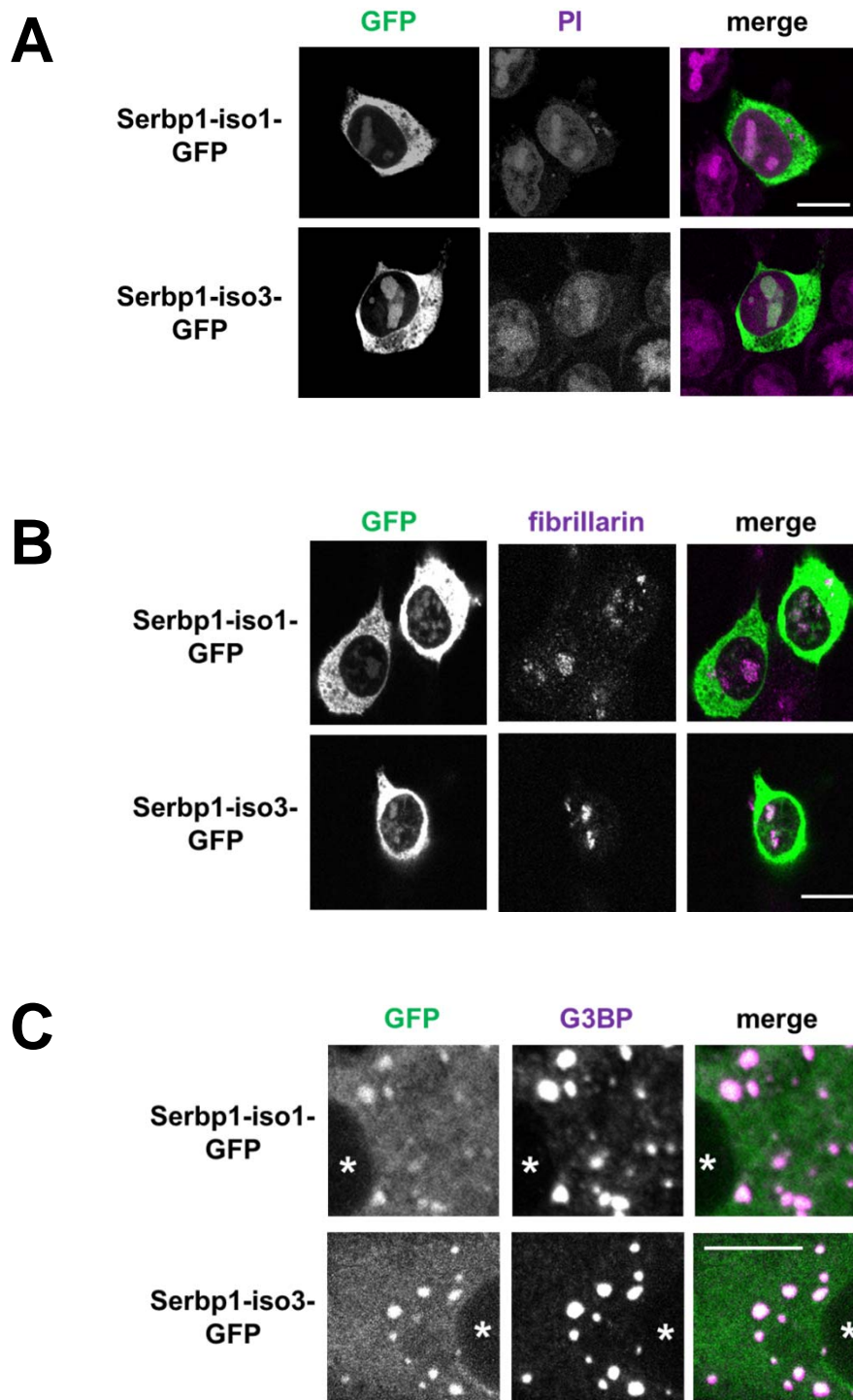
**Supplementary Table S1.** TOF-MS data on Serbp1 (isoform 1) in Figure 4B

Residues	Observed m/z	$M_r$		Delta	Peptide sequence	Peak no. in Figure 4B
		Expected <sup>a</sup>	Calculated			
2 – 16	1684.9218	1683.9145	1683.8151	0.0994	PGHLQEGFGCVVTNR	1
17 – 32	1943.9880	1942.9807	1942.8837	0.0971	FDQLFDDESDPFEVLK	2
112 – 122	1241.6991	1240.6918	1240.6160	0.0758	RPDQQLQGDGK	3
137 – 145	1175.7040	1174.6967	1174.6346	0.0621	RFEKPLEEK	4
217 – 236	2086.0857	2085.0784	2084.9763	0.1021	GGSGSHNWGTVKDELTESPK.	5
327 – 344	2112.0393	2111.0320	2110.9126	0.1194	SKSEEHAEDSVMDHHFR	6
327 – 344	2128.0234	2127.0161	2126.9076	0.1086	SKSEEHAEDSVMDHHFR. (including oxidation (M))	7
329 – 344	1896.8951	1895.8878	1895.7857	0.1022	SEEHAEDSVMDHHFR	8
329 – 344	1912.8772	1911.8699	1911.7806	0.0893	SEEHAEDSVMDHHFR (including oxidation (M))	9

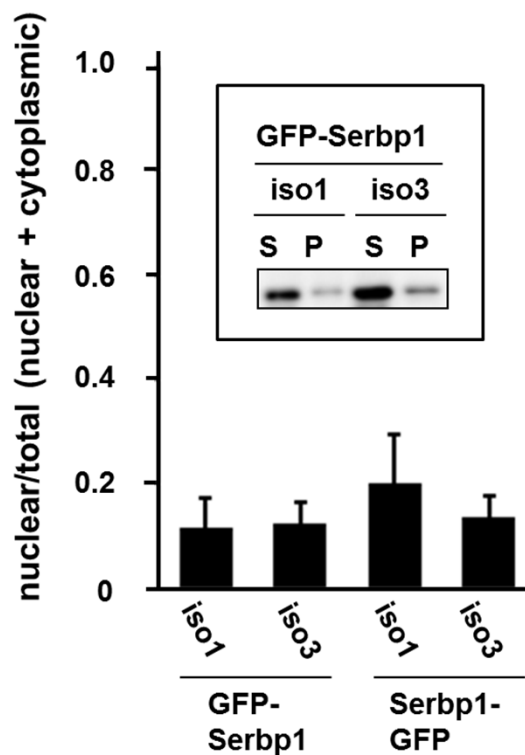
<sup>a</sup>Each experimental m/z value ( $MH^+$ ) was transformed to a relative molecular mass ( $M_r$ ) by the Mascot program. The  $M_r$  values are shown as “Expected  $M_r$ ” in this table.



**Supplementary Figure S1.** Schematic representation of the four isoforms of human Serbp1. Key regions referred to in text and calculated molecular mass of each isoform are indicated (see also Figure 1A). Compared with mouse/rat Serbp1 (Figure 1A), human Serbp1 contains a single histidine insertion (triangles in this figure).



**Supplementary Figure S2.** Intracellular localization of the C-terminally GFP-fused isoforms 1 and 3 of mouse Serbp1. (A) Co-staining of each isoform and nuclei. (B) Co-staining of each isoform and fibrillarin. (C) Co-staining of each isoform and stress granules. The asterisks indicate nuclei. Scale bars, 10  $\mu$ m.



**Supplementary Figure S3.** Subcellular fractionation and localization of the isoforms 1 and 3 of mouse Serbp1. Human 293T cells were transfected with a vector encoding one of the following four proteins: N-terminally GFP-fused isoforms 1 and 3 and C-terminally GFP-fused isoforms 1 and 3. The cells were lysed with Triton X-100 and centrifuged at 10,000 g to obtain the supernatant (cytoplasmic fraction, S) and the nuclear pellet (P). These fractions were subjected to immunoblotting with anti-GFP antibody, and band intensity was measured. The data represent mean  $\pm$  SD (n = 3). An example of the immunoblots is shown in the inset.